

Structural effects on the spin-state transition in epitaxially strained LaCoO₃ films

James M. Rondinelli and Nicola A. Spaldin*

Materials Department, University of California, Santa Barbara, CA, 93106-5050, USA

(Dated: June 15, 2021)

Using density functional theory within the LSDA + U method, we investigate the effect of strain on the spin state and magnetic ordering in perovskite lanthanum cobaltite, LaCoO₃. We show that, while strain-induced changes in lattice parameters are insufficient to stabilize a non-zero spin state, additional heteroepitaxial symmetry constraints – in particular the suppression of octahedral rotations – stabilize a ferromagnetic intermediate-spin state. By comparing with experimental data for the bulk material, we calculate an upper bound on the Hubbard U value, and describe the role that the on-site Coulomb interaction plays in determining the spin-state configuration.

PACS numbers: 71.20.-b, 71.15.Mb, 75.30.Wx, 71.27.+a

I. INTRODUCTION

The desire to control magnetism with external perturbations other than magnetic fields has motivated much recent research on the strain- and electric field-response of magnetic materials.^{1,2,3} Such control might enable future *Mottronic* applications, in which small external perturbations drive transitions between competing electronic, orbital, charge and spin orderings, causing drastic changes in properties. Thin film heterostructures containing transition metal oxides are proving particularly promising in this emerging field; for example, electric-field switching of magnetization has been achieved through exchange-bias coupling of ferromagnetic Co_{0.9}Fe_{0.1} to multiferroic BiFeO₃,⁴ and substrate induced strain has been used to tune magnetic interactions⁵ in magnetoelastic composites (see Ref. 6 for a review). Recent reports^{7,8,9,10} of a substrate-dependent spin state in epitaxial films of LaCoO₃ are of particular interest since they suggest a route to switching magnetism off (low spin diamagnetic d^6 Co³⁺) and on (intermediate- or high-spin Co³⁺).

Lanthanum cobaltite is a rhombohedral ($R\bar{3}c$) perovskite that has been of continued interest for the last half-century, due in part to the many magnetic phase transitions that occur as a function of temperature, pressure and chemical doping.^{11,12,13,14,15} These transitions are a consequence of the competing crystal-field splitting energy (Δ_{CF}), Hund's exchange energy (J_H) and d -orbital valence bandwidth (W), which are similar in magnitude, resulting in low-, intermediate- or high-spin d^6 Co³⁺, depending on the details of the system. In the ground state ($T = 0$ K), LaCoO₃ is a diamagnetic insulator with a low-spin ($S=0$, $t_{2g}^6 e_g^0$) Co³⁺ configuration. It is thermally excited to a paramagnetic intermediate- ($S=1$, $t_{2g}^5 e_g^1$) or high-spin ($S=2$, $t_{2g}^4 e_g^2$) semiconducting state above approximately 95 K.¹⁶ The nature of this spin-state transition is still under debate: inelastic neutron scattering,¹⁷ x-ray absorption spectroscopy (XAS) and magnetic circular dichroism experiments¹⁸ suggest a first-order transition to the high-spin (HS) state, while other x-ray photoemission (XPS) and XAS spectra in addition to electron energy loss (EELS) spectroscopy

suggest the intermediate-spin (IS) state.^{12,19,20,21} Similarly, Hartree-Fock cluster²² and full-potential DFT calculations¹⁵ suggest the HS state is more stable than the IS state, while other LSDA + U calculations obtain the reverse result.^{23,24}

In contrast to the bulk behavior, recent studies on LaCoO₃ thin films report ferromagnetism with a field-cooled magnetization of 0.37 μ_B /Co ion on a substrate that causes 1.84% tensile strain.^{7,8} Although ferromagnetic hysteresis loops have been recorded by several groups,^{7,8,9,10,25} it remains unclear experimentally whether such magnetism is an intrinsic feature of strained LaCoO₃, or whether it arises from sample off-stoichiometry (ferromagnetism induced by hole doping is observed in bulk Sr-rich LaCoO₃ samples),²⁶ or is a surface effect resulting from the change in coordination of surface Co ions (also recently reported in bulk samples).²⁷

In this work, we use *ab-initio* calculations based on density functional theory (DFT) to show that epitaxial strain can indeed drive a spin-state transition to a ferromagnetic state in stoichiometric LaCoO₃. The transition is not caused, however, by strain-induced changes of the lattice constants, but rather relies on interface-induced changes in the tilt pattern of the CoO₆ octahedra.

II. COMPUTATIONAL DETAILS

We use the the projector augmented plane wave (PAW) method of DFT,²⁸ as implemented in the Vienna *Ab Initio* Simulation Package (VASP) code.^{29,30} To accurately describe the exchange and correlation, we use the spherically averaged form of the rotationally invariant local spin density approximation + Hubbard U (LSDA+ U) method^{31,32} with one effective Hubbard parameter $U_{\text{eff}} = U - J$, and treat the double counting term within the fully localized limit. We use the supplied VASP PAW pseudopotentials (LA_S, CO, O_S) with the $5p^6 5d^1 6s^2$ valence configuration for La, $4s^1 3d^8$ for Co, and $2s^2 2p^4$ for O. Other technical details include a plane wave energy cutoff of 550 eV, a $7 \times 7 \times 7$ k -point grid to sample the

Brillouin zone, and the tetrahedron method with Blöchl corrections³³ and an $11 \times 11 \times 11$ k -point grid to calculate the densities of states.

III. BULK LaCoO_3

A. Correlation Effects

The LSDA+ Hubbard U approach has been successful in treating static correlations in transition metal oxides; however the selection of an appropriate U_{eff} is rarely straightforward, and a number of methods exist for determining suitable values. These include experimental measurement from photoemission spectroscopy,³⁴ self-consistent calculations^{35,36,37} and educated guesswork. LaCoO_3 represents a particularly difficult case because of the strong dependence of orbital occupation – which affects the polarizability and screening, and in turn the U_{eff} – on pressure and strain.

Indeed, XPS experiments have found the d - d Coulomb correlations to range from 3.5 to 7.5 eV^{12,38} depending on the structural details of the samples. Previous single-site and two-site configuration-interaction cluster calculations have obtained values from 4 to 5.5 eV.^{12,19} On the other hand, recent first-principles calculations suggest that the spin state is independent of the choice U ,²¹ and values as large as 9 eV have been used to study temperature dependent spin-state transitions.²³ Each method does agree however that the d - d electron repulsion for the low- and intermediate-spin states is approximately the same.

Due to these discrepancies in the literature, in the first part of this study we revisit the effects of electron repulsion on the spin-state and orbital occupation in bulk LaCoO_3 . We begin by calculating the critical U value that induces a spin state transition in the bulk rhombohedral structure by calculating the total energies for each spin state as a function of U_{eff} . Since the bulk zero kelvin state is known to be low spin, this requirement then provides a bound on allowable U_{eff} values for studying the experimentally observed ferromagnetic thin films.

Here we use the low temperature experimental structural parameters found in Ref. 16 ($a = 5.275$ Å, $\alpha = 61.01^\circ$) and fully relax the internal coordinates with $U_{\text{eff}} = 0$ eV until the forces are less than 1 meV Å⁻¹. Within the LSDA, we find the correct ground state structure: a diamagnetic insulator with a 0.45 eV band gap, which is close to the measured optical gap.³⁸ Our calculated energies and magnetic moments as a function of U_{eff} are shown in Figure 1. The most striking finding is that the experimentally observed $S = 0$ ground state is only stable for U_{eff} values less than 4.0 eV. Therefore we regard 4.0 eV as an upper bound on U_{eff} for LaCoO_3 .

In Figure 1(inset) the relative energies of the diamagnetic $S = 0$, IS $S = 1$, and HS $S = 2$ states are also shown. [For these comparison calculations we impose ferromagnetic (FM) order in the IS and HS Co sublattice

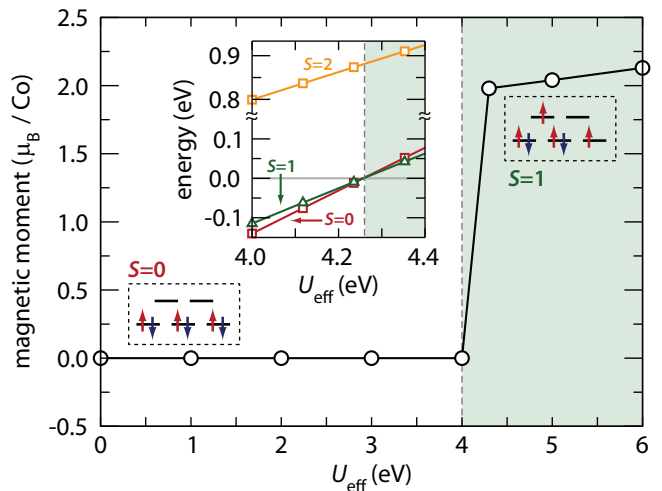


FIG. 1: (Color online) Calculated magnetic moment as a function of U_{eff} in bulk rhombohedral LaCoO_3 with the corresponding orbital energy diagrams. (INSET) Relative energies per formula unit of the $S = 0$, $S=1$ and $S=2$ spin states.

so that we can fix the total spin moment.] As expected, as U_{eff} is increased, spin pairing in the t_{2g} manifold becomes less favorable as the energy gain from the Hund's exchange energy exceeds the energy cost in creating a singlet state and thereby reduces the relative energies of higher spin states. Such correlation-induced spin-state transitions, in which higher U_{eff} values induce states with higher magnetic moments, have previously been found in a number of other transition metal compounds.^{39,40,41,42} Co^{3+} is a particularly interesting case, however, because the low-spin state is non-magnetic and so the spin-state transition increases the magnetic moment to a finite value from an initial value of zero. Interestingly, at the transition to the $S = 1$ state, we find $U_{\text{eff}}/W=0.27$, which is low compared to most moderately- or strongly-correlated magnets; in addition, W is largely independent of U_{eff} (not shown). For all U_{eff} values we find that the HS state is more than 1.0 eV higher in energy than the IS or LS states.

The critical U_{eff} value we have determined with this approach is in good agreement with x-ray photoemission experiments reported in Ref. 38 and recent first-principles calculations in Ref. 43. Therefore, for the remainder of this study, we strictly use values of $U_{\text{eff}} < 4.0$ eV unless noted otherwise. The strong dependence of the ground-state spin configuration on U_{eff} partly explains the inconsistencies between different first-principles calculations in describing the evolution of the spin-state transition.

B. Electronic Structure

Before investigating the effects of strain on the magnetic behavior we describe the nature of the unusual intermediate $S = 1$ state of LaCoO_3 compared to the dia-

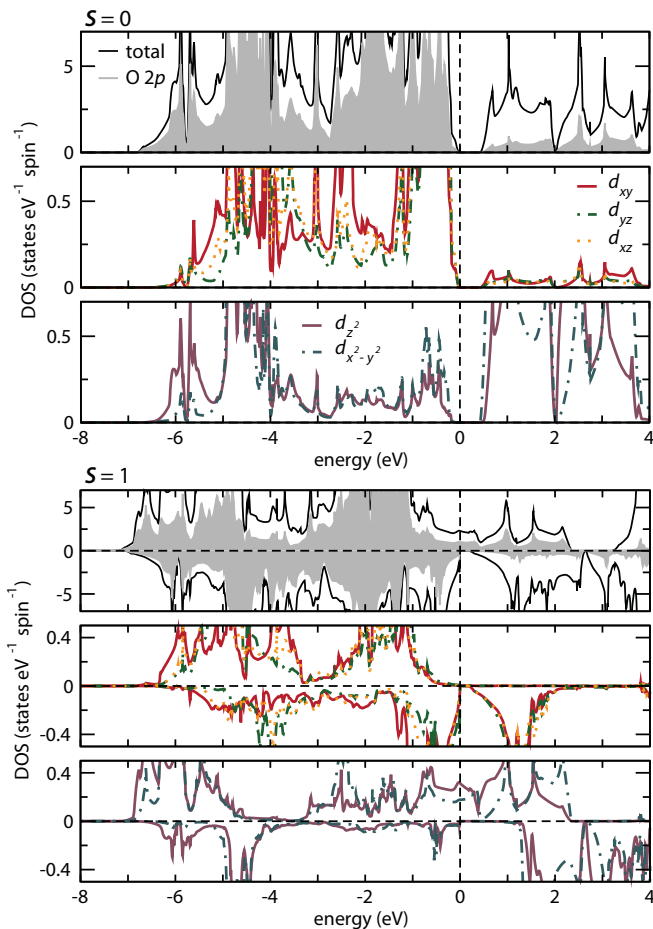


FIG. 2: (Color online) Spin- and orbital-resolved densities of states for $S = 0$ (UPPER) and $S = 1$ (LOWER) rhombohedral LaCoO_3 ($U_{\text{eff}} = 3.0$ eV). In the low-spin state, a diamagnetic insulator is found, while a half-metallic ground state is found with a local magnetic moment of $1.8 \mu_B$ per Co atom in the intermediate spin state.

magnetic $S = 0$ state. In the molecular cluster limit [Figure 1(inset)], when $\Delta_{\text{CF}} > J_{\text{H}}$ the low-spin configuration is favored, while when $\Delta_{\text{CF}} < J_{\text{H}}$ the high-spin state dominates due to the gain in exchange energy from the parallel alignment of spins; the intermediate spin state might be expected when $\Delta_{\text{CF}} \approx J_{\text{H}}$. Furthermore, as evident in Figure 2, hybridization and covalency between the O $2p$ and Co $3d$ states causes dramatic deviations from the simple molecular cluster picture by causing strong broadening of the bands; in particular the Co e_g orbitals span more than 11 eV in energy.

In Figure 2 we show our calculated electronic densities of states for the $S = 0$ and constrained $S = 1$ ferromagnetically ordered LaCoO_3 at the experimental lattice parameter with a $U_{\text{eff}} = 3.0$ eV. In the low-spin state, the Co t_{2g} manifold is fully occupied with triply degenerate d_{xy} , d_{xz} and d_{yz} orbitals; the valence band is formed by a mixture of these Co states and O $2p$ orbitals. The doubly degenerate $d_{x^2-y^2}$ and d_{z^2} orbitals which make up the e_g

manifold form the conduction band.

In the intermediate-spin state, on the other hand, broadening of the band widths causes the majority up-spin e_g band to extend below the Fermi energy, and the minority t_{2g} band to extend above. The hole in the t_{2g} manifold consists of a superposition of the minority $\frac{1}{\sqrt{3}}(d_{xy} + d_{yz} + d_{xz})$ orbitals, and the “missing” electron occupying the lower part of the majority e_g band is in a $\frac{1}{\sqrt{2}}(d_{z^2} + d_{x^2-y^2})$ state. This behavior causes our calculated ferromagnetic intermediate-spin state to be half-metallic. Note, however, that bulk LaCoO_3 is in fact an insulator up to room temperature⁴⁴; we will return to this discrepancy later.

IV. STRAINED LaCoO_3

Spin-state transitions in bulk LaCoO_3 are known to occur as a function of unit cell volume,¹⁶ where the tendency for an excited spin state is favored for larger unit cell volumes due to competition between the energy penalty in forming a singlet state and the gain in Hund’s exchange energy favoring ferromagnetic alignment of spins. This is evidenced by the fact that high spin Co^{3+} has a larger ionic radius (0.61 Å), compared to the low spin Co^{3+} (0.55 Å).⁴⁵ Indeed, this is consistent with our calculations for the ideal cubic perovskite where the LSDA+ U equilibrium volume of the intermediate state is approximately 2% larger than that of the low spin configuration.

In this section we examine likely crystallographic structural distortions in thin films to determine whether they cause a spin-state crossover. In general, heteroepitaxial strain from coherent growth on a substrate with a mismatched lattice constant can modify the structure by changing the lattice parameters, symmetry or chemistry at the interface. Therefore we explore whether computations that incorporate changes in Co–O–Co bond angles, Co–O bond lengths, unit cell volume, or combinations of these effects, are able to reproduce the ferromagnetic state which is observed experimentally in thin film LaCoO_3 .

A. Effect of Changes in Lattice Parameter

The low temperature rhombohedral structure of LaCoO_3 belongs to the ($a^-a^-a^-$) Glazer tilt system, in which successive octahedra rotate in opposite senses along each crystallographic direction. The Co–O–Co bond angle is approximately 166° . The importance of such octahedral rotations on the electronic properties of thin film perovskite oxides has been the subject of many recent reports, particularly in the context of their effect on ferroelectricity.^{46,47} An effect on *magnetic* properties is also likely, because changes in Co–O–Co bond angles can strongly affect the magnetic superexchange interactions. In this section we investigate whether strain-

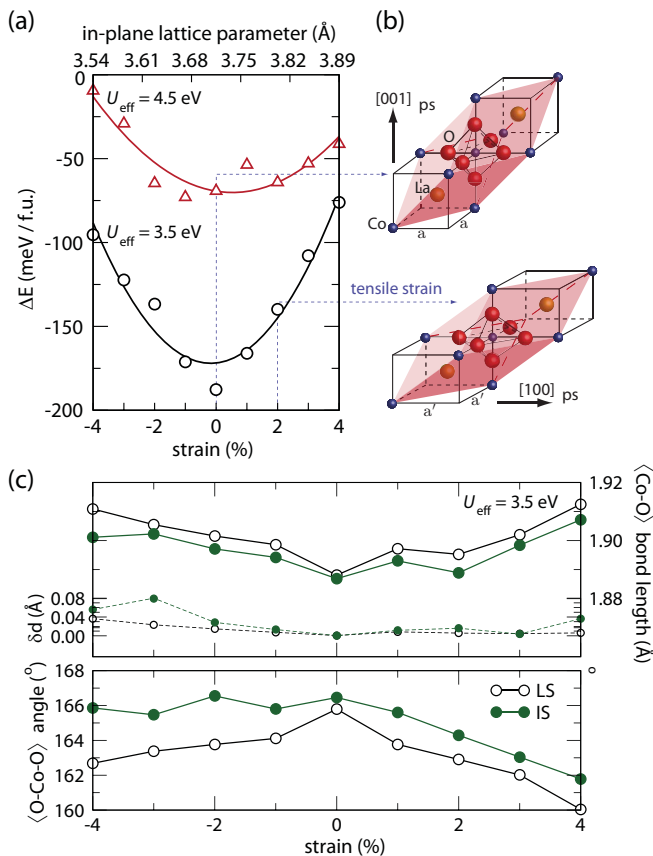


FIG. 3: (Color online) (a) Energy difference between the diamagnetic low-spin and ferromagnetic intermediate-spin states, ΔE , as a function of epitaxial strain applied in the pseudo-cubic (ps) (100) plane of the rhombohedral structure (b) shown relative to the cubic perovskite. (c) The relaxed mean Co-O bond lengths, bond differences δd between the long- and short bonds in the CoO_6 octahedra, and the O-Co-O bond angles for $U_{\text{eff}} = 3.5\text{eV}$. The lines are a guide for the eye.

induced changes in these bond angles are sufficient to stabilize the intermediate-spin state.

In Figure 3(a), we plot our calculated energy difference between low- and intermediate-spin states with ferromagnetic order as a function of strain applied to the pseudo-cubic (100) plane with respect to the LSDA equilibrium volume. Values are shown for two U_{eff} values, 3.5 and 4.5 eV, chosen to be above and below the critical U_{eff} value of 4.0 eV that we established in the previous section. (The high spin state is not shown, since it is ~ 1 eV higher in energy at all strain values.) At each in-plane strain value we adjust the out-of-plane lattice parameter and rhombohedral angle to maintain the bulk equilibrium volume, then fully relax the atomic positions. We find that, for U_{eff} below our calculated critical value, the low-spin ground state is stable up to strains of 4%; therefore we predict that strain-induced changes in lattice parameters alone are insufficient to cause a spin-state transition in LaCoO_3 up to reasonable strain values. Even our un-

physically large U_{eff} of 4.5 eV does not induce a transition to the intermediate spin state until just beyond 4% compressive strain. The half-metallic state remains stable until strain values above 3% ($U_{\text{eff}} = 3.5$ eV) and 1% ($U_{\text{eff}} = 4.5$ eV), when the electronic structure becomes fully metallic.

To understand the absence of spin-state transition with strain, we plot in Figure 3(c) the evolution of the mean Co-O bond length and the mean Co-O-Co bond angle as a function of strain for $U_{\text{eff}} = 3.5$ eV. With either compressive or tensile strain, the average Co-O bond length increases from the equilibrium (zero-strain) value. All bond lengths increase uniformly, however, such that the CoO_6 octahedra remains perfectly octahedral, and the ideal O_h crystal field is maintained. This is supported by the bond length differences between the long- and short-Co-O bonds (δd) in the CoO_6 octahedra. We find significant changes in the Co-O-Co bond angles, particularly for tensile strain. In many magnetic perovskites, such large changes in bond angles are sufficient to change the magnetic ordering.^{48,49} We believe that the absence of spin crossover in this case is due to the exceptionally broad bandwidth of the Co e_g orbitals, which reduces the exchange energy gain from spin polarization.

B. Effect of Octahedral Rotations and Distortions

Next we isolate the influence of these octahedral rotations by manually disabling them while applying strain. Our motivation is two-fold. First, there is experimental evidence suggesting that LaCoO_3 grows in such a ‘cube-on-cube’ manner on many substrates.^{7,8,50} Second, disabling the octahedral rotations causes the system to respond to strain by changing the local symmetry around the Co ion; therefore we can examine the influence of the crystal field on the spin-state transition.

The no-rotations constraint is imposed by using a five atom unit cell which prohibits rotations by symmetry; as a side-effect this also imposes ferromagnetic ordering. (We later examine if this is indeed the preferred magnetic ordering.) We begin by setting the in-plane pseudo-cubic lattice parameter (a) to that of the experimental substrate $(\text{LaAlO}_3)_{0.3}(\text{Sr}_2\text{AlTaO}_6)_{0.7}$ (LSAT) value (3.87 Å) with the optimized LSDA+ U volume ($c/a = 0.955$), and relax the internal coordinates and out-of-plane (c) lattice constant; the resulting structure is diamagnetic and 270 meV higher in energy than the LSDA equilibrium $R\bar{3}c$ LS structure.

Next, we apply uniaxial strain by varying the c/a ratio with a fixed to the experimental LSAT value, and show the resulting calculated magnetic moment in Figure 4. Our main finding is that, at the experimental c/a ratio, the IS state is lower in energy than the LS, and therefore we predict that the Co ions should be magnetic. The origin of the stabilization of the intermediate state is the lifting of the octahedral crystal field by the tetragonal symmetry adopted when the octahedral rota-

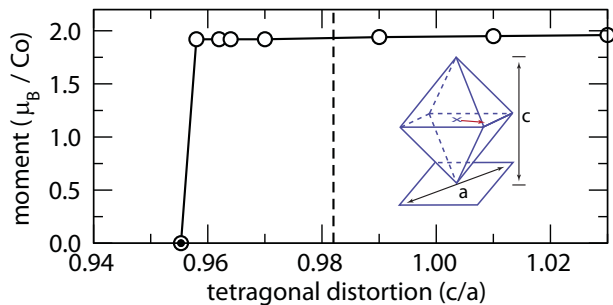


FIG. 4: (Color online) Calculated magnetic moment as a function of c/a for tetragonal LaCoO_3 with a fixed to the experimental LSAT lattice parameter (3.87 Å). The dashed line (filled circle) indicates the experimental (LSDA equilibrium) c/a ratio. (INSET) Schematic representation of Co displacement within the equatorial octahedral plane (arrow).

	c/a	FM	A-AFM	G-AFM
LSDA+ U	0.955	0.0 (0.0)	n/a (0.0) ^a	+147 (2.8)
Exp.	0.982	0.0 (1.9)	+375 (2.7)	+180 (2.8)

^aWe were unable to converge the A-type AFM arrangement.

TABLE I: Total energy differences (in meV) for various magnetic orderings within the tetragonal crystal structure relative to the five atom ferromagnetic unit cell. Values are given at the experimental and optimized LSDA+ U c/a ratios. Calculated magnetic moments per Co atom in μ_B are given in parentheses.

tions are disabled. Small ($< 1\%$) uniaxial expansion of the out-of-plane lattice constant modifies the tetragonal crystal field splitting sufficiently to favor occupation of the e_g manifold. In contrast, when octahedral rotations are allowed, strain is accommodated through changes in the rotation angles rather than through modification of the local bond lengths around the Co ions; the local crystal field splitting is therefore largely unchanged and the diamagnetic state remains stable.

Next we investigate whether the ferromagnetic order imposed so far for computational convenience is indeed the lowest energy magnetic ordering by comparing its energy with those of the A-type antiferromagnetic (A-AFM), and G-type antiferromagnetic (G-AFM) orderings for this structure. The total energies for each structure are shown in Table I for both the experimental and optimized LSDA+ U c/a values. The energies are given relative to the FM single unit cell configuration. We find that the G-AFM and A-AFM structures are 180 and 375 meV per formula unit higher in energy than the ferromagnetically ordered intermediate spin state at the experimental c/a ratio. This is consistent with the experimentally observed ferromagnetism.

Intriguingly, the structure with disabled octahedral rotations relaxes to a polar space group ($C2/c$) with the Co^{3+} ion moving 0.06 Å off-center in the ab plane. By summing the formal ionic charges multiplied by their dis-

placements from their centrosymmetric positions we find an in-plane polarization of $17.5 \mu\text{C}/\text{cm}^2$ at the experimental $c/a = 0.982$ ratio. Note that since our overall electronic ground state is metallic, we are unable to evaluate the electronic contribution to the polarization using the standard Berry's phase approach. Indeed the onset of ferroelectric polarization caused by the disabling of octahedral rotations in perovskite oxides has been noted in a number of calculations, and is believed to result from the off-centering of ions to maintain a favorable bond order.^{46,47} However, since our electronic structure is overall metallic, we cannot predict ferroelectric behavior.

V. DISCUSSION

While our finding of ferromagnetism is consistent with recent experimental reports, there are some important differences between our computations and the experimental observations. First, and analogous to the bulk intermediate-spin case, our calculated tetragonal structure is half-metallic, with a broad majority spin O $2p$ - Co e_g band crossing the Fermi level; experimentally the ferromagnetic films are found to be insulating. In addition, the sizes of most measured magnetic moments are an order of magnitude smaller than our calculated value. Recent x-ray magnetic circular dichroism (XMCD) experiments on thin films, however, find a local Co moment of $1.2 \mu_B$, which is in better agreement with our calculations.¹⁰

In this last section we attempt to reconcile our finding of a strain-induced half-metallic ferromagnetic arrangement with experimental reports of insulating LaCoO_3 on LSAT. In particular, we explore likely Jahn-Teller distortions and orbital orderings which are known to allow both ferromagnetism and insulating behavior in oxides.⁵¹ We also examine the effect of including spin-orbit interactions in our calculations, since these couplings can make significant contributions to determining the orbital occupation in many transition metal oxides.

The possibility of an orbitally ordered state in LaCoO_3 was suggested previously in Ref. 23, and unrestricted Hartree-Fock calculations on similar materials⁵² found that small Jahn-Teller structural distortions can stabilize an insulating state. Cooperative Jahn-Teller distortions (ranging from 1 to 6% from low to room temperature) have indeed been demonstrated in LaCoO_3 with various techniques including high-resolution x-ray diffraction,⁵³ Raman scattering,⁵⁴ and neutron diffraction.^{55,56} Ref. 53 obtained a monoclinic structure with $I2/a$ symmetry, consistent with the A-AFM ordering seen in LaMnO_3 .

Although the TYPE-A monoclinic structure was investigated previously in Ref. 23, we revisit the possible orbital ordering available in strained LaCoO_3 by imposing from 1-6% Jahn-Teller structural distortions of the CoO_6 . In the same way, we study TYPE-D ordering (space group $P4/mbm$), which has uniform orbital occupation along the c -direction and alternating orbital occupation in the

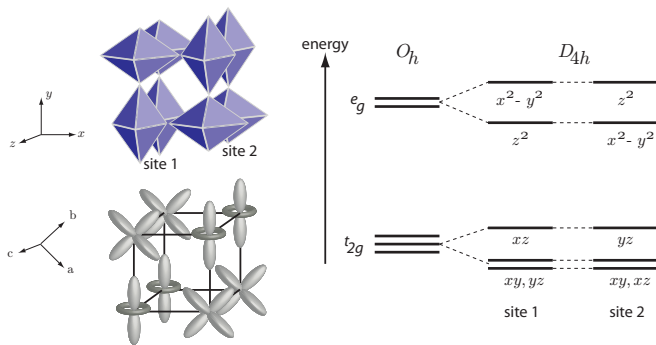


FIG. 5: The TYPE-D Jahn-Teller distorted structure is shown with the possible e_g orbital ordering configuration. The orbital degeneracy is also split at each of the two sites, according to the orientation of the elongation of the oxygen octahedra with respect to the c lattice parameter.

ab -plane, consistent with overall ferromagnetic superexchange (Figure 5). This 2D antiferrodistortive behavior allows for $d_{x^2-y^2}$ and d_{z^2} orbital ordering due to the splitting of the e_g degeneracy from the structural distortions of the oxygen octahedra. Similarly the threefold degenerate t_{2g} orbitals also split into a two-fold degeneracy, that is lower in energy than the single non-degenerate state. In all cases examined no e_g orbital order is observed, in spite of the imposed octahedral structural distortions. Due to the degeneracy of the Co e_g states at the Fermi level, although the density of states is reduced, a half-metallic ferromagnetic state persists. In contrast, the higher energy G-AFM structure considered earlier is insulating.

Finally, we examine the effect of spin-orbit interactions in LaCoO_3 , since such coupling of the magnetic spin degrees of freedom to the lattice can change the relative level splitting and degeneracy of spin and orbital ground states in the $3d$ transition metal oxides.^{57,58} For the diamagnetic $S = 0$ configuration we find that spin-orbit interaction has a negligible effect on the electronic structure as expected for a filled t_{2g} manifold. On the other hand, in a recent theoretical study⁴³ it was suggested the $S = 1$ state does show significant changes in the electronic structure near the Fermi level when spin orbit interactions are included. In contrast to those results which used a generalized-gradient approximation (GGA+ U) for the exchange-correlation functional, we do not find significant deviations in the electronic structure when spin-orbit coupling is included in the calculations. This result is likely due to the difference in the description of our starting intermediate spin-state configurations: we begin with a half-metallic ground state, whereas in Ref. 43, a fully metallic state is found with a high density of states at the Fermi level. When spin-orbit coupling is included in the calculation, the large peak feature is naturally split into a doublet.

The origin of the two inconsistencies – our half-metallic

rather than insulating ground state, and larger magnetic moment per Co ion compared with experiment – might lie in the difficulties associated with producing and characterizing high quality, uniform transition metal oxide films, or from a failure of the LSDA+ U method to fully describe the complex orbital physics. Future theoretical investigations should consider more sophisticated methods such as dynamical mean field theory, in which dynamical correlations (spin fluctuations) can in principle be treated explicitly. Indeed, recent inelastic neutron scattering measurements report a small Jahn-Teller distortion which has short-range dynamical character.^{55,59} This dynamic Jahn-Teller effect is consistent with a proposed vibronic $e^1\text{-O-}e^0$ superexchange between intermediate-spin Co atoms,²⁷ and would allow for fluctuations of AFM exchange which should reduce the magnetic moment. On the experimental front, our calculations suggest that more detailed characterization of the *local* electronic and structural properties will be invaluable in understanding and exploiting the spin behavior of LaCoO_3 films.

VI. CONCLUSIONS

In summary, by comparing our calculated LSDA+ U spin state of bulk LaCoO_3 with the measured low temperature behavior, we have determined a critical upper bound of 4 eV on the Hubbard U parameter for LSDA+ U calculations for LaCoO_3 . Using our critical U value, we have established that strain-induced changes in lattice parameters are insufficient to cause transitions to finite magnetic moment spin states at reasonable values of strain. Instead, if the cooperative octahedral tiltings and rotations are deactivated, intermediate-spin local moments are stabilized on the Co ions at small strain values, and these order ferromagnetically. Our results suggest a possible route to dynamically controlling magnetism using an electric field, in superlattices of LaCoO_3 with a piezoelectric material.

Acknowledgments

We thank A.J. Hatt, R. Seshadri, T. Saha-Dasgupta, Y. Suzuki and J.W. Freeland for valuable discussions. This work was supported by the NSF under the grant NIRT 0609377 (NAS) and a NDSEG fellowship sponsored by the DoD (JMR). Portions of this work made use of MRL Central Facilities supported by the MRSEC Program of the National Science Foundation (DMR05-20415), the CNSI Computer Facilities at UC Santa Barbara (CHE-0321368), and the National Center for Supercomputing Applications under grant no. TG-DMR-050002S and utilized the SGI Altix COBALT system.

- * Address correspondence to: nicola@mrl.ucsb.edu
- 1 R. Ramesh and N. A. Spaldin, *Nature Materials* **6**, 21 (2007).
 - 2 A. Brinkman, M. Huijben, M. van Zalk, J. Huijben, U. Zeitler, J. C. Maan, W. G. van der Wiel, G. Rijnders, D. H. A. Blank, and H. Hilgenkamp, *Nat. Mater* **6**, 493 (2007).
 - 3 H. Yamada, Y. Ogawa, Y. Ishii, H. Sato, M. Kawasaki, H. Akoh, and Y. Tokura, *Science* **305**, 646 (2004).
 - 4 Y.-H. Chu, L. W. Martin, M. B. Holcomb, M. Gajek, S.-J. Han, Q. He, N. Balke, C.-H. Yang, D. Lee, W. Hu, et al., *Nature Mater.* **7**, 478 (2008).
 - 5 H. Yamada, M. Kawasaki, T. Lottermoser, T. Arima, and Y. Tokura, *Appl. Phys. Lett.* **89**, 052506 (2006).
 - 6 W. Eerenstein, N. D. Mathur, and J. Scott, *Nature* **44**, 759 (2006).
 - 7 D. Fuchs, C. Pinta, T. Schwarz, P. Schweiss, P. Nagel, S. Schuppler, R. Schneider, M. Merz, G. Roth, and H. v. Löhneysen, *Phys. Rev. B* **75**, 144402 (2007).
 - 8 D. Fuchs, E. Arac, C. Pinta, S. Schuppler, R. Schneider, and H. v. Löhneysen, *Phys. Rev. B* **77**, 014434 (2008).
 - 9 A. Herklotz, A. D. Rata, L. Schultz, and K. Dörr, *ArXiv e-prints* **805** (2008), 0805.0991.
 - 10 J. W. Freeland, J. X. Ma, and J. Shi, *Appl. Phys. Lett.* **93**, 212501 (2008).
 - 11 J. Goodenough, *J. Phys. Chem. Solids* **6**, 287 (1958).
 - 12 T. Saitoh, T. Mizokawa, A. Fujimori, M. Abbate, Y. Takeda, and M. Takano, *Phys. Rev. B* **55**, 4257 (1997).
 - 13 M. Medarde, C. Dallera, M. Grioni, J. Voigt, A. Podlesnyak, E. Pomjakushina, K. Conder, T. Neisius, O. Tjernberg, and S. N. Barilo, *Phys. Rev. B* **73**, 054424 (2006).
 - 14 G. Vankó, J.-P. Rueff, A. Mattila, Z. Németh, and A. Shukla, *Phys. Rev. B* (2006).
 - 15 K. Knížek, Z. Jiráček, J. Hejtmánek, and P. Novák, *J. Phys.: Condens. Matter* **18**, 3285 (2006).
 - 16 P. G. Radaelli and S.-W. Cheong, *Phys. Rev. B* **66**, 094408 (2002).
 - 17 A. Podlesnyak, S. Streule, J. Mesot, M. Medarde, E. Pomjakushina, K. Conder, A. Tanaka, M. W. Haverkort, and D. I. Khomskii, *Phys. Rev. Lett.* **97**, 247208 (2006).
 - 18 M. W. Haverkort, Z. Hu, J. C. Cezar, T. Burnus, H. Hartmann, M. Reuther, C. Zobel, T. Lorenz, A. Tanaka, N. B. Brookes, et al., *Phys. Rev. Lett.* **97**, 176405 (2006).
 - 19 M. Abbate, J. C. Fuggle, A. Fujimori, L. H. Tjeng, C. T. Chen, R. Potze, G. A. Sawatzky, H. Eisaki, and S. Uchida, *Phys. Rev. B* **47**, 16124 (1993).
 - 20 S. Masuda, M. Aoki, Y. Harada, H. Hirohashi, Y. Watanabe, Y. Sakisaka, and H. Kato, *Phys. Rev. Lett.* **71**, 4214 (1993).
 - 21 R. F. Klie, J. C. Zheng, Y. Zhu, M. Varela, J. Wu, and C. Leighton, *Phys. Rev. Lett.* **99**, 047203 (2007).
 - 22 M. Zhuang, W. Zhang, and N. Ming, *Phys. Rev. B* **57**, 10705 (1998).
 - 23 M. A. Korotin, S. Y. Ezhov, I. V. Solovyev, V. I. Anisimov, D. I. Khomskii, and G. A. Sawatzky, *Phys. Rev. B* **54**, 5309 (1996).
 - 24 S. K. Pandey, A. Kumar, S. Patil, V. R. R. Medicherla, R. S. Singh, K. Maiti, D. Prabhakaran, A. T. Boothroyd, and A. V. Pimpale, *Phys. Rev. B* **77**, 045123 (2008).
 - 25 C. Pinta, D. Fuchs, M. Merz, M. Wissinger, E. Arac, H. v. Löhneysen, A. Samartsev, P. Nagel, and S. Schuppler, *Phys. Rev. B* **78**, 174402 (2008).
 - 26 M. A. Señarís-Rodríguez and J. B. Goodenough, *J. Solid State Chem.* **118**, 323 (1995).
 - 27 J.-Q. Yan, J.-S. Zhou, and J. B. Goodenough, *Phys. Rev. B* **70**, 014402 (2004).
 - 28 P. E. Blöchl, *Phys. Rev. B* **50**, 17953 (1994).
 - 29 G. Kresse and J. Furthmüller, *Phys. Rev. B* **54**, 11169 (1996).
 - 30 G. Kresse and D. Joubert, *Phys. Rev. B* **59**, 1758 (1999).
 - 31 V. I. Anisimov, F. Aryasetiawan, and A. I. Liechtenstein, *J. Phys.: Condens. Matter* **9**, 767 (1997).
 - 32 S. L. Dudarev, G. A. Botton, S. Y. Savrasov, C. J. Humphreys, and A. P. Sutton, *Phys. Rev. B* **57**, 1505 (1998).
 - 33 P. E. Blöchl, O. Jepsen, and O. K. Andersen, *Phys. Rev. B* **49**, 16223 (1994).
 - 34 A. Fujimori, I. Hase, H. Namatame, Y. Fujishima, Y. Tokura, H. Eisaki, S. Uchida, K. Takegahara, and F. M. F. de Groot, *Phys. Rev. Lett.* **69**, 1796 (1992).
 - 35 V. I. Anisimov and O. Gunnarsson, *Phys. Rev. B* **43**, 7570 (1991).
 - 36 M. Cococcioni and S. de Gironcoli, *Phys. Rev. B* **71**, 035105 (2005).
 - 37 G. K. H. Madsen and P. Novák, *Europhys. Lett.* **69**, 777 (2005).
 - 38 D. D. Sarma, N. Shanthi, S. R. Barman, N. Hamada, H. Sawada, and K. Terakura, *Phys. Rev. Lett.* **75**, 1126 (1995).
 - 39 S. Lebègue, S. Pillet, and J. G. Ángyán, *Phys. Rev. B* **78**, 024433 (2008).
 - 40 P. Werner and A. J. Millis, *Phys. Rev. Lett.* **99**, 126405 (2007).
 - 41 T. Tsuchiya, R. M. Wentzcovitch, C. R. S. da Silva, and S. de Gironcoli, *Phys. Rev. Lett.* **96**, 198501 (2006).
 - 42 P. Baettig, C. Ederer, and N. A. Spaldin, *Phys. Rev. B* **72**, 214105 (2005).
 - 43 S. K. Pandey, A. Kumar, S. Banik, A. K. Shukla, S. R. Barman, and A. V. Pimpale, *Phys. Rev. B* **77**, 113104 (2008).
 - 44 Y. Tokura, Y. Okimoto, S. Yamaguchi, H. Taniguchi, T. Kimura, and H. Takagi, *Phys. Rev. B* **58**, R1699 (1998).
 - 45 W. Koehler and E. Wollan, *J. Phys. Chem. Solids* **2**, 100 (1956).
 - 46 D. J. Singh and C. H. Park, *Phys. Rev. Lett.* **100**, 087601 (2008).
 - 47 A. J. Hatt and N. A. Spaldin, *Appl. Phys. Lett.* **90**, 242916 (2007).
 - 48 M. A. Subramanian, A. P. Ramirez, and W. J. Marshall, *Phys. Rev. Lett.* **82**, 1558 (1999).
 - 49 M. Retuerto, M. Garcia-Hernandez, M. J. Martinez-Lope, M. T. Fernandez-Diaz, J. P. Attfield, and J. A. Alonso, *J. Mater. Chem.* **17**, 3555 (2007).
 - 50 Y. Suzuki, private communication.
 - 51 T. Mizokawa, D. I. Khomskii, and G. A. Sawatzky, *Phys. Rev. B* **60**, 7309 (1999).
 - 52 T. Mizokawa and A. Fujimori, *Phys. Rev. B* **51**, 12880 (1995).
 - 53 G. Maris, Y. Ren, V. Volotchaev, C. Zobel, T. Lorenz, and T. T. M. Palstra, *Phys. Rev. B* **67**, 224423 (2003).
 - 54 A. Ishikawa, J. Nohara, and S. Sugai, *Phys. Rev. Lett.* **93**,

- 136401 (2004).
- ⁵⁵ D. P. Kozlenko, N. O. Golosova, Z. Jiráček, L. S. Dubrovinsky, B. N. Savenko, M. G. Tucker, Y. L. Godec, and V. P. Glazkov, *Phys. Rev. B* **75**, 064422 (2007).
- ⁵⁶ D. Phelan, J. Yu, and D. Louca, *Phys. Rev. B* **78**, 094108 (2008).
- ⁵⁷ H. Wu, Z. Hu, D. I. Khomskii, and L. H. Tjeng, *Phys. Rev. B* **75**, 245118 (2007).
- ⁵⁸ T. Maitra and R. Valentí, *Phys. Rev. Lett.* (2007).
- ⁵⁹ D. Phelan, D. Louca, S. Rosenkranz, S.-H. Lee, Y. Qiu, P. J. Chupas, R. Osborn, H. Zheng, J. F. Mitchell, J. R. D. Copley, et al., *Phys. Rev. Lett.* **96**, 027201 (2006).